JOURNAL OF MATERIALS SCIENCE 31 (1996) 2591–2598

Cellular decomposition in Fe–26Ni–(2–3)Ti–Nb steels with an addition of aluminium or molybdenum

J. JELEŃKOWSKI
Department of Materials Science and Engineering, Warsaw University of Technology, ul. Narbutta 85, 02-524 Warsaw, Poland

Cellular η decomposition in three Fe–26Ni–(2–3)Ti–Nb type steels was investigated. One of these steels was alloyed with molybdenum while the two others, differing in grain size, contained an addition of aluminium. In Ni26AlTi3Nb and Ni26MoTi2Nb steels quenched from 1223 K in water, the first colonies of η decomposition were observed after holding for 4 h at 923 K. A longer holding at this temperature resulted in growth of η decomposition cells in the steel with molybdenum while in the steels with aluminium, a halting of the decomposition and the appearance of isolated plates of the η phase was observed. In Ni26MoTi2Nb and Ni26Al2Ti3Nb steels, quenched in water and subsequently cold treated in liquid nitrogen, repeated heating in the temperature range 293–999.9 K at a rate of 2.5, 10 and 40 K min^{-1} and cooling at a rate 320 K min^{-1} favoured the cellular η decomposition more markedly in the steel with molybdenum. On cooling to room temperature, austenite within the decomposition cells transformed into martensite. The tendency to cellular decomposition depended to a higher degree on the factors which stabilize austenite as well as on the presence of precipitates in grain boundaries, than on the grain size.

1. Introduction

In the investigations [1–10] devoted to the cellular decomposition of high-nickel austenite, involving the precipitation of the η-Ni_3Ti phase, it has been concluded that besides the chemical driving force, originating from supersaturation, other stimuli for the decomposition also exist, namely recrystallization caused by stresses which appear during the decomposition process [4], migration of grain boundaries [5, 6], and a tendency to decrease the energy of interphase boundaries by the precipitation of a new phase [7, 8]. Of all the causes involved, migration of grain boundaries played the most important role in the decomposition process. Theoretically [9], decomposition can take place if the migrating boundary is convex, i.e. directed towards the interior of the grain. If the migrating boundary is concave, allotropic precipitates can be formed. The cellular decomposition in Ni30Ti6 steel takes place [1] in two clearly separated temperature ranges. It starts at 673 K at primary grain boundaries and propagates with the rise in temperature. Plates of the η-Ni_3Ti phase have a coherent boundary with austenite, the following crystallographic relationships being maintained: $(0\,0\,0\,1)\,Ni_3Ti \parallel (1\,1\,1)\gamma$ and $[0\,\bar{1}\,\bar{1}\,0]\,Ni_3Ti \parallel [1\,\bar{1}\,0]$. Holding at 973 K, which constitutes the final stage of heating, favours the renewed decomposition at former grain boundaries, the plates of the η phase being now thicker and (as regards their composition and crystallographic structure) nearer to the Laves phase, $(Fe,Ni)_2Ti$.

Precipitates of the η phase, which are formed during the prolonged holding, resemble the Widmannstätten structure [4] while those occurring during the rapidly proceeding process of continuous decomposition have the shape of cubes [11]. In each case, the growth of the η phase is accompanied by the dissolution of the γ′ phase.

In Fe–Ni–Ti alloys also, a cellular decomposition with the participation of the γ′ phase was observed, but it differed from the η decomposition by a fan-shaped arrangement of plates. This decomposition is controlled by diffusion along the migrating grain boundaries. It is initiated by spherical particles of the γ′ phase, situated in the neighbourhood of grain boundaries [10–12].

The interest in investigating the cellular decomposition is justified by its advantageous effect on mechanical properties of Fe–Ni–Ti alloys. This process is competitive with relation to the continuous decomposition, i.e. it weakens the strengthening of the matrix by the γ′ phase [10, 13–15]. At a differentiated grain size, it initially extends over fine-grain regions [16]. A complete decomposition can probably be achieved only in recrystallized reversed austenite [17]. Austenite in decomposition cells can transform into martensite isothermally or athermally without affecting the morphology of the η plates [13, 17–19]. During

0022–2461

the martensitic transformation in decomposition cells in Fe–Ni–Ti alloys, defect density increases more markedly than during the $\gamma \rightarrow \alpha'$ transformation in non-ageing alloys [10]. During cold treatment, a considerably greater quantity of martensite is formed as compared with that appearing after the η decomposition. The high degree of dispersion of phases constituting the cells and the disappearance of primary austenite grain boundaries are, from the view-point of the microstructure arising from the cellular η decomposition, additional advantages.

The possibility of improving mechanical properties by the cellular η decomposition, as established by several authors [11, 16, 17, 21], was a stimulus for undertaking the investigation of this process in experimental melts of Fe–Ni–Ti steels in which the structure is, as a rule, composed of large and small grains. An addition of small amounts of aluminium or molybdenum to these steels exerts an essential effect on the mechanism of ageing as well as on the martensitic transformation and the reverse transformation [22]. Mechanical properties of Ni26MoTi2Nb and Ni26Al2Ti3Nb steels after selected heat-treatment processes performed under laboratory conditions [22, 23] are tabulated in Table I. Mechanical properties of Ni26AlTi3Nb steel were not determined.

2. Experimental procedure

The investigations were performed on experimental melts of the chemical composition given in Table II. The chromium as well as copper content did not exceed 0.02%. The steels were melted in a vacuum induction furnace. Ingots, weighing 20 kg each, were subjected to homogenization for 10 h at 1373 K and then forged into bars of 16 mm diameter. After homogenizing, the bars were broached to transform them into wires of 4 mm diameter.

The investigations were carried out using calorimetric specimens of 3 mm diameter and 2 mm thick, subjected to austenitizing for 1 h at 1223 K in a vacuum furnace, followed by quenching in water. Specimens of Ni26MoTi2Nb and Ni26AlTi3Nb steels were aged in a calorimeter for 4–7 h at 923 K. Heating up to 923 K, as well as cooling, was conducted at a rate of 40 K min^{-1}. Specimens, quenched and cold treated for 0.5 h in liquid nitrogen, were subjected (in the same calorimeter) to cyclic heating and cooling in the temperature range 293–999.9 K. The rate of heating was 2.5, 10 and 40 K min^{-1} and that of subsequent cooling 320 K min^{-1}. The highest temperature of the cycle constituted the upper limit of the measuring range of the calorimeter and was a little lower than the A_f temperature of the steels involved.

Calorimetric curves used for determining critical temperatures of the $\alpha' \rightarrow \gamma$ transformation were recorded during each heating and cooling cycle of the specimens contained in the Perkin–Elmer DSC-2 calorimeter. The specimens were previously quenched in water and cold treated in liquid nitrogen. As a standard sample, ARMCO iron was used.

After heat treatment, microscopic examinations were performed. Microsections for the examination on a light microscope were prepared by mechanical and electrolytic polishing and etched with a reagent containing 15 ml HNO_3, 5 ml HCl and 2.5 g $CuCl_2$. Foils to be examined on a Jeol 100B microscope were thinned using the Struers device. The specimens were next subjected to hardness measurements (Hanemann tester) as well as to X-ray analysis (Philips diffractometer) and magnetometric phase analysis (Förster magnetometer).

TABLE I Proportion of martensite and mechanical properties of steels Ni26MoTi2Nb and Ni26Al2Ti3Nb after selected heat-treatment processes

Designation	Condition[a]	Proportion of martensite (%)	Tensile strength, R_m (MPa)	Proof stress, $R_{0.2}$ (MPa)	Elongation, A_{10} (%)
Ni26MoTi2Nb	A	0	360	190	64
	B	0	680	380	47
	C	61	960	695	15
	D	30	1980	1890	11
	E	35	1490	1005	18
Ni26Al2Ti3Nb	A	0	380	185	58
	B	0	1020	710	45
	C	72	970	685	14
	D	20	1780	1700	5
	E	28	1245	670	11

[a] A, after quenching in water; B, after cooling in air to room temperature; C, after cold treating in liquid nitrogen; D, after cold treating in liquid nitrogen and holding for 2 h in the temperature range of the reverse transformation; E, after strengthening by the reverse transformation at a heating rate of 20 K min^{-1} and subsequent cooling in air.

TABLE II Chemical composition (wt %)

	C	S	P	Si	Mn	Ni	Ti	Al	Mo	Nb
Ni26MoT2Nb	0.02	0.009	0.007	0.11	0.17	26.0	2.15	0.04	1.15	0.11
Ni26Al2Ti3Nb	0.03	0.006	0.004	0.18	0.18	25.5	3.25	2.09	0.06	0.35
Ni26AlTi3Nb	0.04	0.006	0.005	0.16	0.11	26.4	3.00	0.68	0.02	0.19

3. Results and discussion

The M_s temperature of the steels involved did not exceed 223 K, after homogenizing and quenching in water. That is why specimens of Ni26MoTi2Nb and Ni26AlTi3Nb steels, subjected to austenizing and water quenching, had austenitic structure while the structure of Ni26MoTi2Nb and Ni26Al2Ti3Nb steel specimens was martensitic austenitic, after quenching and cold treating in liquid nitrogen, the proportion of martensite being, respectively, 58% and 62%.

A_s and A_f temperatures of the steels involved as determined from the first heating to 999.9 K, are tabulated in Table III. Calorimetric curves recorded during the second heating showed an increase in critical temperatures of the reverse transformation. Calorimetric records obtained for further heating processes (particularly for steel containing aluminium at heating rates of 2.5 and 10 K min^{-1}) did not deviate markedly from the base line and were not analysed.

TABLE III Critical temperatures of the transformation at the first heating to 999.9 K. Values exceeding 1000 K were obtained by extrapolation.

Steel	Heating rate (K min^{-1})					
	2.5		10		40	
	A_s	A_f	A_s	A_f	A_s	A_f
Ni26MoTi2Nb	740	~1028	738	988	740	973
Ni26Al2Ti3Nb	745	~1033	735	~1026	726	~1020

3.1. Cellular decomposition in aged specimens

After electrolytic polishing, annealing twins were observed in the structure of supersaturated austenite, their proportion amounting in all the steels involved to ~15%. During mechanical polishing of the steel with aluminium, strain-induced plate martensite was formed in some grains while in the vicinity of grain boundaries, martensite-free zones remained (Fig. 1a). In the steel with molybdenum, strain-induced martensite of the butterfly-type appeared at twin boundaries (Fig. 1b). The grain size corresponded, according to the ASTM scale, to nos 6–10 in steels with aluminium and to nos 5–6 in steel with molybdenum.

3.1.1. Ni26MoTi2Nb steel

Irrespective of the mode of polishing applied, microsections of the specimens of this steel became lustreless. At first at grain boundaries and then within the grains, single plates and plate packs of martensite were formed (Fig. 2a). After about a month the whole polished surface was covered with a relief. After etching, the structure shown in Fig. 2b was observed. The proportion of the ferromagnetic phase, as revealed by a ferrite meter, was ~1%, while that of martensite, determined by X-ray analysis, amounted to ~43%.

The first regions of the cellular η decomposition in this steel were observed after ageing for 4 h at 923 K. A decomposition colony in bright field is shown in Fig. 3a and that in dark field, in the $(0\,1\,\bar{1}\,0)\eta$ reflection, in Fig. 3b. Fig. 3c represents the diffraction pattern of interfering reciprocal lattices of austenite and

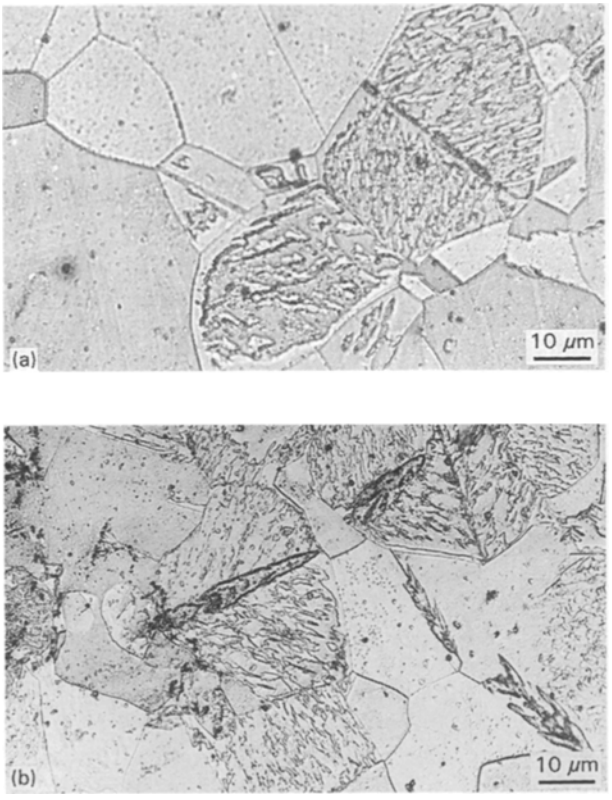

Figure 1 (a) Strain-induced martensite and martensite-free boundaries in Ni26AlTi3Nb steel and (b) strain-induced martensite of the butterfly-type at twin boundaries in Ni26Mo2Ti3Nb steel.

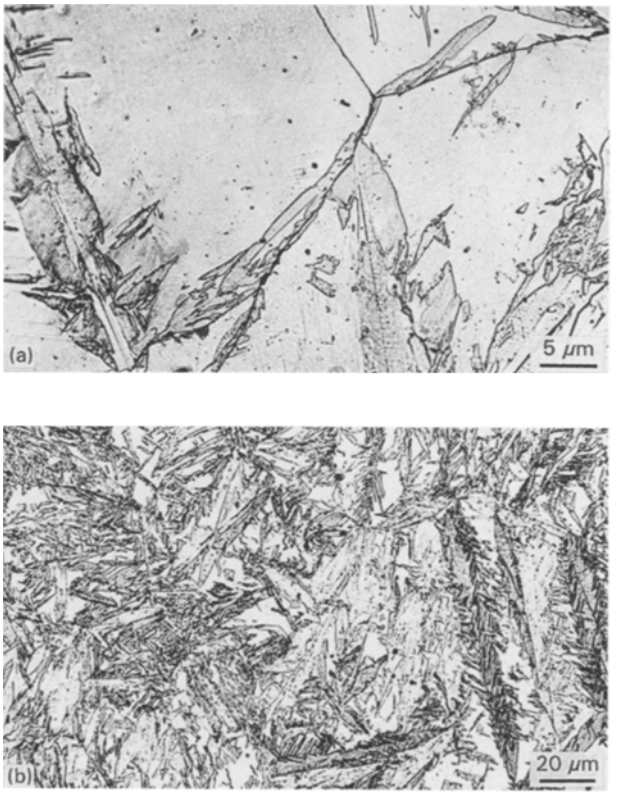

Figure 2 Surface martensite in Ni26MoTi2Nb steel, (a) 1 week and (b) 1 month after polishing.

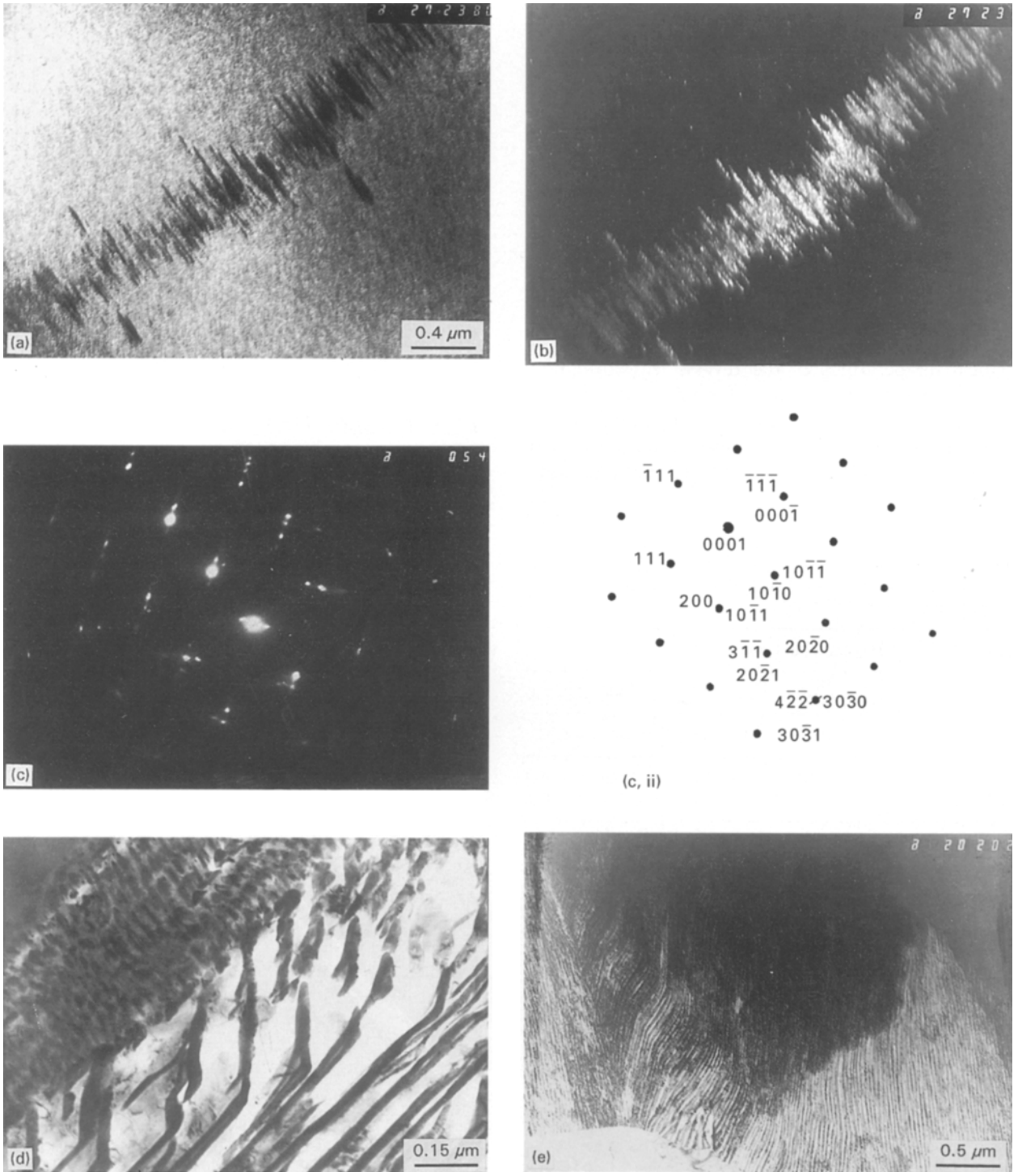

Figure 3 Colony of the cellular η decomposition in Ni26MoTi2Nb steel after ageing for 4 h at 923 K, in (a) bright field, (b) dark field in the (1 0 1 0) η reflection, (c) diffraction pattern and index from this region. (d, e) Colonies of (d) η and γ′ cellular decomposition, and (e) those of cellular η decomposition, after ageing for 7 h at the same temperature.

the η phase. It shows the following crystallographic relationships between the η phase and austenite: $(0\,0\,0\,1)\eta \parallel (1\,1\,1)\gamma$ and $(1\,0\,\bar{1}\,0)\eta \parallel (2\,\bar{1}\,\bar{1})\gamma$. The coexistence of cellular η and γ′ decomposition was also observed (Fig. 3d).

After ageing for 7 h, the cells of the η decomposition assumed a typical morphology, characteristic of them (Fig. 3e). Aged specimens cooled down to room temperature contained 2% martensite after ageing for 4 h and 28% martensite after ageing for 7 h. They differed markedly as regards hardness (Table IV)). Hardness values were determined from 12 or so indentations made for a single phase or a phase mixture. The level of confidence was adopted as equal to 0.95.

3.1.2. Ni26AlTi3Nb steel

After ageing for 4 h at 923 K, the morphology of this steel (Fig. 4a) differed essentially from that shown in Fig. 1a. The microstructure of these steels contained 66% lenticular and thin-plate martensite while the remainder was aged residual austenite. The initial stage of the cellular η decomposition after ageing for 4 h is shown in Fig. 4b. After ageing for 7 h, the

TABLE IV Microstructure, surface microhardness and percentage of martensite (in parentheses) in aged specimens

Condition of the specimen	Type of microstructure	$HV_{0.02}$ hardness	
		Ni26AlTi3Nb	Ni26MoTi2Nb
Quenching from 1223 K in water	Austenite	197 ± 7	238 ± 8
	Surface martensite	255 ± 8(0.1)	198 ± 5(1.0)
After quenching and ageing for 4 h at 923 K	Retained austenite + thin-plate martensite	532 ± 25(66)	330 ± 10(2)
	Lenticular martensite	584 ± 22	315 ± 10
As above, but ageing for 7 h	Retained austenite + thin-plate martensite	620 ± 25(75)	483 ± 20(28)
	Plate martensite	639 ± 30	536 ± 25

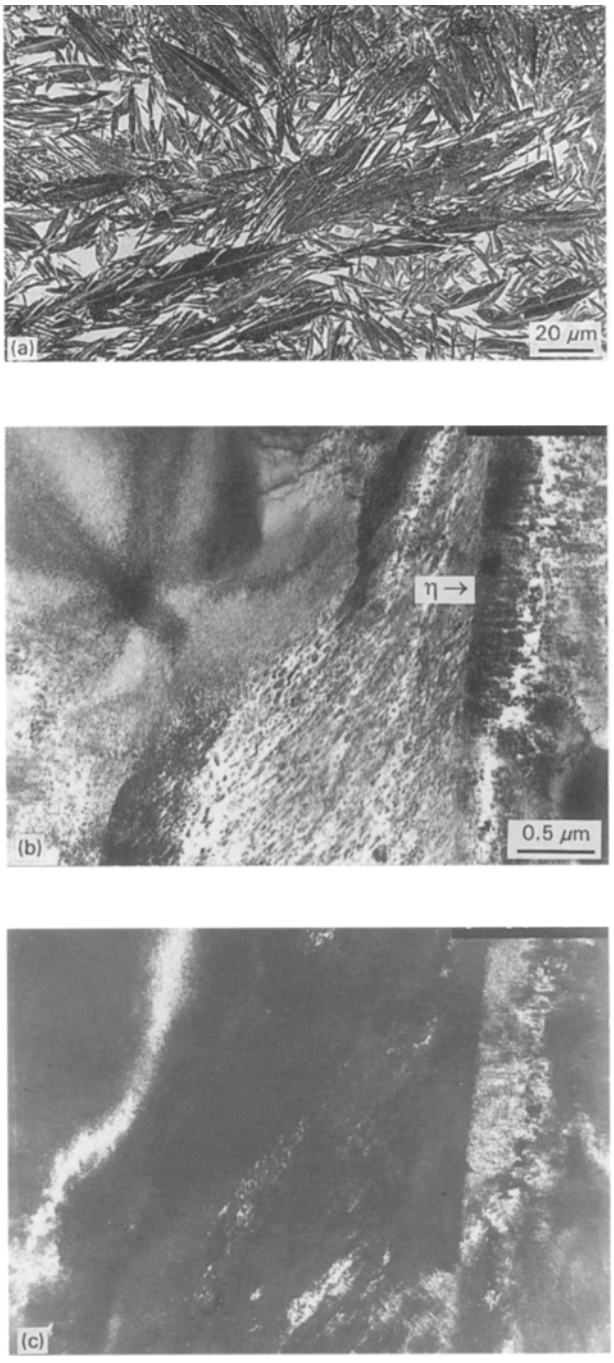

Figure 4 (a) Microstructure of Ni26AlTi3Nb steel after ageing and cooling to room temperature. (b, c) Colonies of η decomposition after ageing for 4 h (b) in bright field and (c) in dark field in the (0 0 0 1) η reflection.

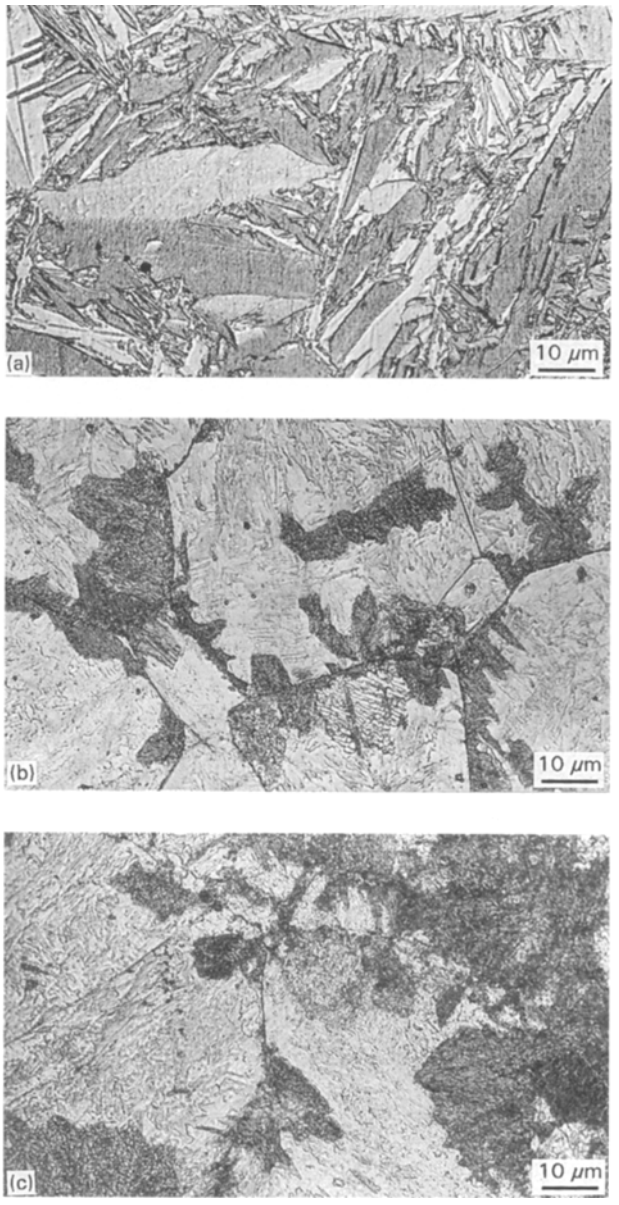

Figure 5 Microstructure of Ni26MoTi2Nb steel: (a) after cold treating, (b, c) after three repeated heatings to 999.9 K at a rate of (b) 2.5 K min^{-1} and (c) 40 K min^{-1}.

regions undergoing the cellular η decomposition were not essentially larger (Fig. 4c), but the proportion of martensite after cooling rises, as a result of destabilization of austenite, to 75%. γ′ decomposition cells were not observed.

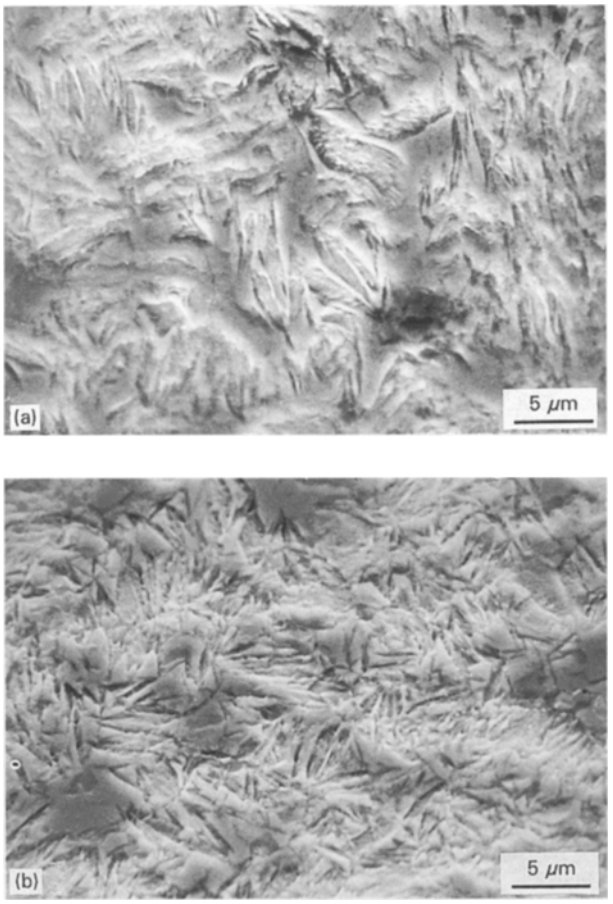

Figure 6 Scanning electron micrographs of Ni26MoTi2Nb steel after three repeated heatings to 999.9 K at a rate of (a) 2.5 K min^{-1} and (b) 40 K min^{-1}.

Taking into account the proportion of martensite in the structure of aged specimens as well as the values of the M_s temperature for specimens with previously homogenized austenite, it is concluded that an addition of aluminium accelerates the continuous γ' decomposition and slows down the cellular η decomposition. An impoverishment of austenite in nickel, aluminium and niobium entails a rise of the M_s temperature markedly above room temperature. In the steel with molybdenum, i.e. with an element which has a lower activity than aluminium, the cellular η decomposition is slowed down to a lesser degree and the effect of the ageing process on the rise of the M_s temperature is not so accentuated.

Under the ageing conditions applied, the cellular η decomposition in Ni26AlTi 3Nb steel, similarly as the cellular γ' decomposition in the steel with molybdenum, has a very restricted extent.

3.2. Cellular decomposition in specimens subjected to cyclic heating and cooling

3.2.1. Ni26MoTi2Nb steel

The first cellules of the η decomposition in the steel with molybdenum were observed after the second thermal cycle. After the third cycle they already extended over considerable areas in the vicinity of primary grain boundaries of austenite. Further thermal cycles did not essentially change the microstructure. This suggests that in the third cycle, equilibrium has been attained between the susceptibility of austenite to the cellular η decomposition and that to the continuous γ' decomposition.

Fig. 5 shows the microstructure of this steel after cold treating in liquid nitrogen (Fig. 5a) and after three times repeated heating at a rate of 2.5 and 40 K min^{-1} to 999.9 K followed by cooling to room temperature (Fig. 5b and 5c). The microstructure of the same specimen, as revealed by scanning microscopy after etching with a reagent containing copper chloride, is shown in Fig. 6a and 6b. The relief seen in scanning electron micrographs testifies to the fact that, on cooling to room temperature, plate martensite is formed in the colonies of the η decomposition. The proportion of martensite, as determined by the magnetometric method, decreased with increasing heating rate, from 20% at a rate of 2.5 K min^{-1} to 16% at a rate of 40 K min^{-1} (Table V).

3.2.2. Ni26Al2Ti3Nb steel

The η decomposition process observed in this steel was similar to that in the steel with molybdenum, but its intensity was weaker.

The microstructure after three thermal cycles involving heating to 999.9 K at rates of 2.5 and 40 K min^{-1} is shown in Fig. 7b and 7c. As may be seen, the localization of the cellular η decomposition differs here from that occurring in the steel with molybdenum. The reason is a more marked inhomogeneity of grain size, resulting from the segregation of alloying elements (Fig. 7a). In contrast to Ni26MoTi2Nb steel, a more accentuated slowing down effect of the heating rate on the extent of the η decomposition was observed (Table V).

TABLE V Proportion of martensite after the reverse transformation involving several heating rates and after the first cooling to room temperature. $HV_{0.1}$ values in parentheses

Steel	After quenching in H_2O	After heating at		
		2.5 K min^{-1}	10 K min^{-1}	40 K min^{-1}
Ni26MoTi2Nb	Austenite (202 ± 4)			
Ni26Al2Ti3Nb	Austenite (284 ± 6)			
	After quenching in liquid N_2			
Ni26MoTi2Nb	58% (223 ± 8)	20% (345 ± 6)	18%	16% (337 ± 5)
Ni26Al2Ti3Nb	62% (307 ± 10)	18% (509 ± 10)	10%	7% (469 ± 10)

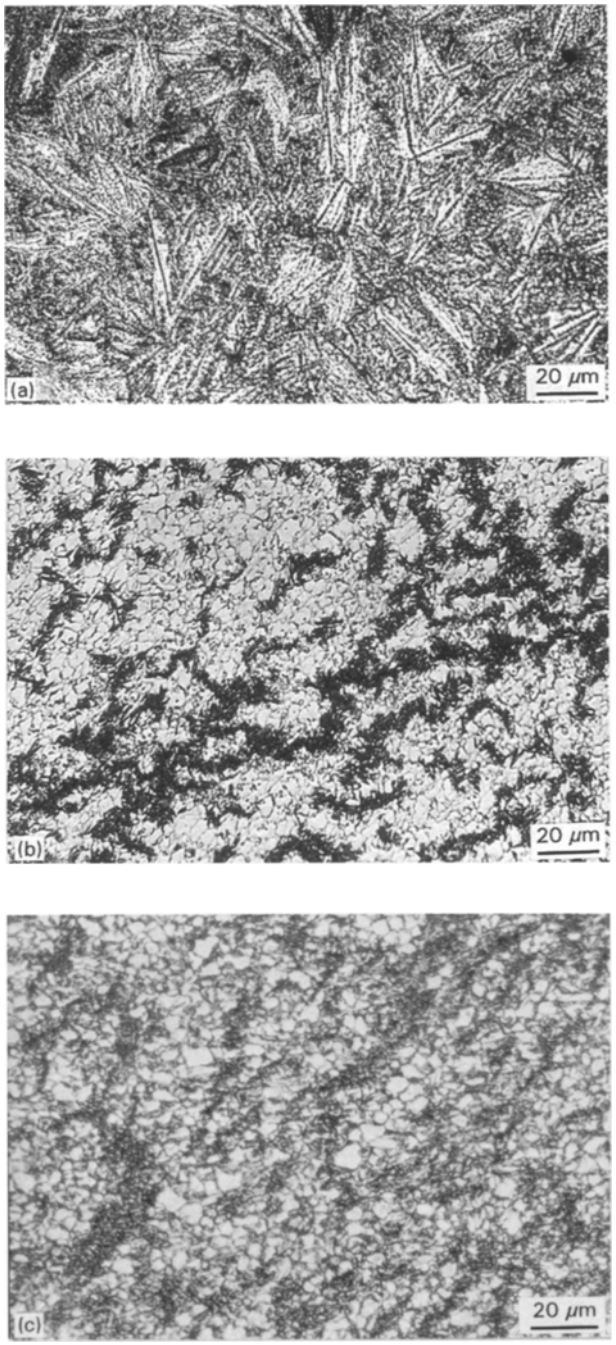

Figure 7 Microstructure of Ni26Al2Ti3Nb steel, (a) after cold treating in liquid nitrogen, (b, c) after three repeated heatings to 999.9 K at a rate of (b) 2.5 K min^{-1} and (c) 40 K min^{-1}.

Scanning electron microscope images represented in Fig. 8a and b show a relief reflecting highly dispersed plate martensite. The decreasing proportion of martensite in the structure is associated with the strengthening of austenite by ageing and phase hardening, which becomes more intense with increasing heating rate.

In thin foils, plates of the η phase were also observed in an arrangement resembling the Widmanstätten structure (Fig. 9a), separated by austenite-containing particles of the γ′ phase. The arrangement of the plate particles and the disposition of the γ′ phase reproduce the orientation of twin crystals of plate martensite from which they have been formed (Fig. 9b).

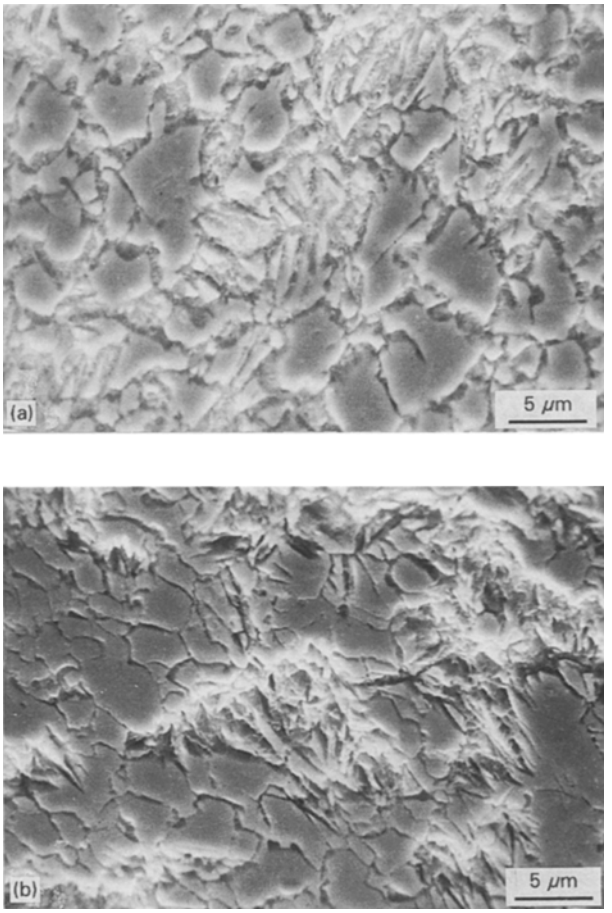

Figure 8 Scanning electron micrographs of Ni26Al2Ti3Nb steel after three repeated heatings to 999.9 K at a rate (a) 2.5 K min^{-1} and (b) 40 K min^{-1}.

Taking into account the proportion of martensite in the initial structure of both steels, as well as the difference in the values of the A_f temperatures, it can be stated that an addition of aluminium activates the continuous γ′ decomposition and slows down the cellular η decomposition. An impoverishment of reversed austenite in nickel, aluminium and niobium entails a rise of the M_s temperature above room temperature. An addition of molybdenum, i.e. of an element which has a lower activity than aluminium, causes the cellular η decomposition to become competitive in relation to the continuous γ′ decomposition. The effect of ageing processes on the rise of the M_s temperature is, in this case, a weaker one.

As compared with ageing, phase hardening occurring as a result of cyclic temperature changes in the range 293–999.9 K, accelerates both kinds of decomposition. However, an increase in heating rate slows down the cellular η decomposition.

In order to establish the proportion of volume undergoing the cellular η decomposition, which transforms into martensite, measurements of the content of retained martensite and secondary martensite should be made. In view of the predominant role of primary grain boundaries, it is hardly possible to establish which kind of austenite, i.e. retained or reversed austenite, shows a stronger tendency to undergo the cellular decomposition.

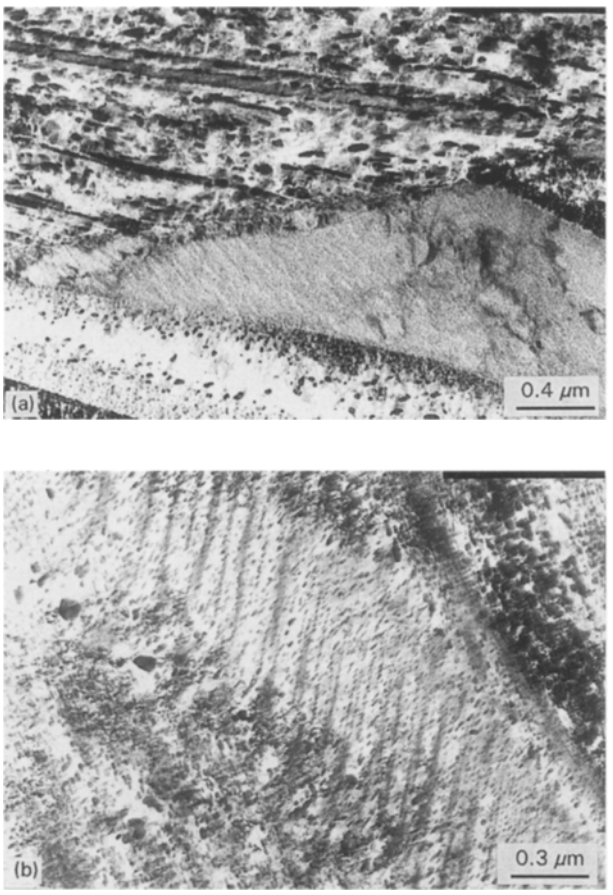

Figure 9 Plate-like particles of the η phase in (a) austenite-containing precipitates of the γ′ phase, and (b) in the parent twin martensite crystal in Ni26Al2Ti3Nb steel subjected to cold treatment and three repeated heatings to 999.9 K.

4. Conclusions

1. An addition of aluminium to Fe–26Ni–(2–3) Ti–Nb steels activates the continuous γ′ decomposition and, as a result, hinders the cellular η decomposition. In contrast to that, an addition of molybdenum causes the cellular η decomposition to be competitive with regard to the continuous γ′ decomposition, particularly after phase hardening.

2. The first η decomposition cells appear in Ni26Al Ti3Nb steel after ageing for several hours, whereupon their growth is rapidly stopped. During longer holding at the ageing temperature, i.e. during ageing by the continuous γ′ decomposition, plates of the η phase occur which, however, do not form decomposition colonies. In the steel with molybdenum, η decomposition cells grow continuously and slowly until their growth is stopped as a result of impoverishment of the titanium in the matrix.

3. In Ni26MoTi2Nb steel, two crystallographic relations between the η phase and austenite in decomposition cells exist, namely $(0\,0\,0\,1)\eta \parallel (1\,1\,1)\gamma$ and $(1\,0\,\bar{1}\,0)\eta \parallel (2\,\bar{1}\,\bar{1})\gamma$.

4. Phase hardening resulting from the martensitic transformation and the reverse transformation as well as from further twice repeated thermal cycles in the temperature range 293–1000 K, strongly accelerates the continuous γ′ decomposition in the steel with aluminium, and thus impedes the cellular η decomposition. In the steel with molybdenum subjected to the same heat treatment, both decomposition processes are competitive, the continuous γ′ decomposition, however, being predominant.

5. In both steels, η decomposition cells transform, during cooling to room temperature, into plate martensite.

References

1. G. R. SPEICH, *Alloy Trans. AIME* **227** (1963) 754.
2. R. K. PITLER and G. S. ANSELL, *Trans. ASM* **57** (1969) 220.
3. S. FLOREEN, *Metall. Rev.* **12** (1968) 115.
4. H. K. HARDY and T. J. HEAL, in "Progress in Metal Physics", Vol. 5 edited by B. Chalmers and R. King (Pergamon Press, London 1954) (in Russian, Metallurgizdat, Moskva, 1958, Vol. 2, p. 285).
5. JU. A. SKAKOV, K. V. VARLI and G. S. MILOVZOROV, *Izv. AN SSSR, S. Fiz.* **34** (1970) 1570.
6. R. A. FOURNELL and J. B. CLARK, *Metall. Trans.* **3** (1972) 2757.
7. K. N. TU and D. TURNBULL, *Acta Metall.* **17** (1969) 1263.
8. K. N. TU, *Metall. Trans.* **3** (1972) 2769.
9. H. I. AARONSON and H. W. AARON, *ibid.* **3** (1972) 2743.
10. V. F. SUKHOVAROV, "Prerivistoye vydieleniye faz v splavach" (Izd. Nauka, Novosibirsk, 1983).
11. V. V. SAGARADZE and A. I. UVAROV, "Uprochnienye austenitnykh staley" (Izd. Nauka, Moscow, 1989).
12. G. HAUSCH and H. WARLIMONT, *Acta Metall.* **21** (1973) 401.
13. D. M. MUZYKA, in "The Superalloys", edited by C. T. Sims and W. C. Hagel (Wiley, New York, 1972) p. 125.
14. N. D. ZEMCOVA and K. A. MALYSHEV, *Phys. Met. Metallov.* **35** (1973) 1006.
15. N. D. ZEMCOVA, K. A. MALYSHEV and E. I. STARCHENKO, *ibid.* **48** (1979) 375.
16. K. A. MALYSHEV, V. V. SAGARADZE *et al.*, "Fazovyj naklop austenitnykh splavov na zhelezoniklevoy osnovye" (Izd. Nauka, Moscow, 1982).
17. V. V. KOKORIN, "Martensitnyje prevrashchenya v neodnorodnykh tvjordykh rastvorach" (Izd. Naukova Dumka, Kiev, 1987).
18. S. JIN and D. HUANG, *Metall. Trans.* **7A** (1976) 745.
19. I. G. KABANOVA, N. D. ZEMCOVA and V. V. SAGARADZE, *Phys. Met. Metallov*, **58** (1984) 344.
20. V. D. SADOVSKIY, N. D. ZEMCOVA and E. I. STARCHENKO, *Dokl. An SSSR* **200** (1981) 88.
21. G. H. BOGACHEVA, V. D. SADOVSKIY and V. M. SHCHASTLIVCEV, *Phys. Met. Metallov.* **23** (1967) 283.
22. J. JELEŃKOWSKI, *Mater. Sci. Technol.* **10** (1994) 1073
23. *Idem, Arch. Nauki. Mater.* (in Polish) **4** (1995) t.18, 296.

Received 25 April
and accepted 23 November 1995